Pergamon

Int. J. Rock Mech. Min. Sci. & Geomech. Abstr. Vol. 33, No. 5, pp. 539–542, 1996

0148-9062/96 $15.00 + 0.00

PII: S0148-9062(96)00004-6

Technical Note

An Improved Wing Crack Model for the Deformation and Failure of Rock in Compression

P. BAUD†
T. REUSCHLɇ§
P. CHARLEZ¶

INTRODUCTION

Brittle materials usually contain small cracks. When loaded in compression these cracks propagate until their interactions lead to final failure. Conventional theories do not currently offer a satisfactory explanation of such a phenomenon. The main problem lies in the fact that there is a contradiction between microstructural and macroscopic behaviours with regard to rupture [1]. Moreover, experiments show that the critical stress, in terms of rupture, is not reproducible for identical samples and loading configurations. This is due to pre-existing small defects which produce high stress concentrations. Numerous theoretical models have been applied to this problem such as purely macroscopic methods using the classical Mohr–Coulomb criterion [2] or other methods using bifurcation theory [3,4]. A first step towards the description of the evolution of a population of cracks is to look at the conditions of propagation of a single crack. A second step is to look at the mechanical interactions between the cracks and their effects on the propagation conditions. A last step will be to derive the macroscopic deformation tensor from the evolution of all cracks. This paper focuses on the first step of this approach, that is, we examine the conditions and the geometry of single crack propagation under biaxial compression. Several solutions have been proposed to solve this problem by looking at the stress intensity factor in mode I [5–8]. An original approximation is presented in this paper which relies on the computation of the stress intensity factor and allows extended numerical applications in view of the next step of our approach.

CRACK PROPAGATION MODEL

We look at the propagation conditions for a crack of length $2a$ subjected to stresses σ_V and σ_H and lying at an angle β with σ_H (Fig. 1). We will focus on the case of biaxial compression, that is $\sigma_V \leqslant 0$ and $\sigma_H \leqslant 0$, the major compressive stress σ_V being vertical. Knowing σ_V, σ_H and β, it is straightforward to derive the shear (σ_T) and normal (σ_N) stresses acting on the crack plane:

$$\sigma_N = \tfrac{1}{2}\{(\sigma_V + \sigma_H) + (\sigma_V - \sigma_H)\cos 2\beta\}$$
$$\sigma_T = \tfrac{1}{2}(\sigma_V - \sigma_H)\sin 2\beta. \quad (1)$$

Since the crack is closed due to the compressive normal stress, we introduce μ, the coefficient of friction. The effective shear stress is thus equal to $|\sigma_{eff}| = |\sigma_T| - \mu|\sigma_N|$. The only stress intensity factor which appears at the crack tip is the mode II factor K_{II} given by $K_{II} = \sigma_{eff}\sqrt{\pi a}$. When the effective shear stress reaches a critical value, the crack begins to propagate but not in its own plane: a wing crack grows from the tip of the initial crack (Fig. 1) in a direction θ for which the transformed mode I stress intensity factor $k'_I(\theta)$ is at a maximum and greater than K_C, the critical stress intensity factor in mode I. The transformed factor is given by [9]:

$$k'_I(\theta) = -\tfrac{3}{2}K_{II}\sin\theta\cos\frac{\theta}{2} \quad (2)$$

which leads to $\theta = \pm 70.5°$ for the direction of initiation of the wing crack, the positive or negative orientation depending on the sign of K_{II}.

In order to determine further wing crack propagation conditions, we assume that the wing crack path is defined by the condition of maximum stress intensity factor K_I at the crack tip. This is equivalent to the condition $K_{II} = 0$ discussed by Cotterell and Rice [10]. The exact calculation of the stress intensity factor at the wing crack tip has been addressed by Nemat-Nasser and Horii [11], and Horii and Nemat-Nasser [5], but their derivation is very difficult to use for computational purposes. So we have to look at approximate models for the wing crack system to make these calculations easier. The problem is that the wing crack is not a straight crack but a curved one the orientation of which depends on its length. Overcoming this hindrance implies some simplifications. The first one is that we replace the curved crack by a straight one by simply connecting the wing crack tip to the main crack tip (Fig. 2). Thus, the orientation θ of the

†Rock and Ice Physics Laboratory, Research School of Geological and Geophysical Sciences, University College London, Gower Street, London WC1E 6BT, U.K.
‡EOPGS, URA 1358, Laboratoire de Physique des Matériaux, 5 rue René Descartes, 67084 Strasbourg Cedex, France.
§Author to whom correspondence should be addressed.
¶TOTAL, 24 cours Michelet, 92069 Parix Cedex 47, France.

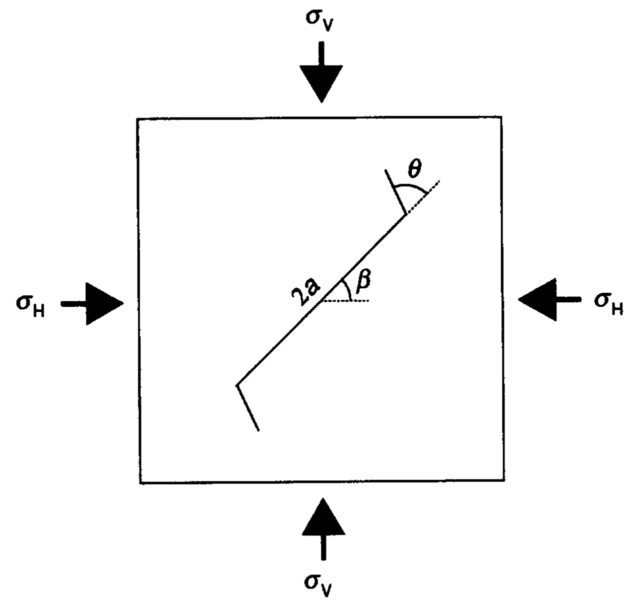

Fig. 1. Sketch illustrating the propagation geometry of a sliding crack under compression.

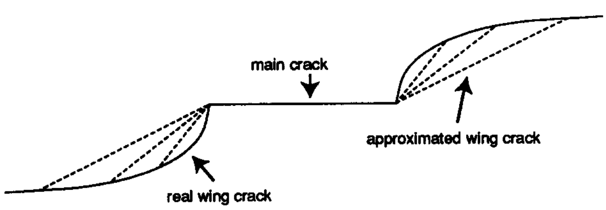

Fig. 2. The real wing crack is replaced by a straight one the orientation of which θ depends on its length.

straight wing crack depends on its length l. This is quite different from the approximation made by Ashby and Hallam [7] since these authors assume that the straight wing crack has a fixed orientation (parallel to the major applied compressive stress) from the initiation. This is not true for short wing cracks and should be kept in mind for later discussion.

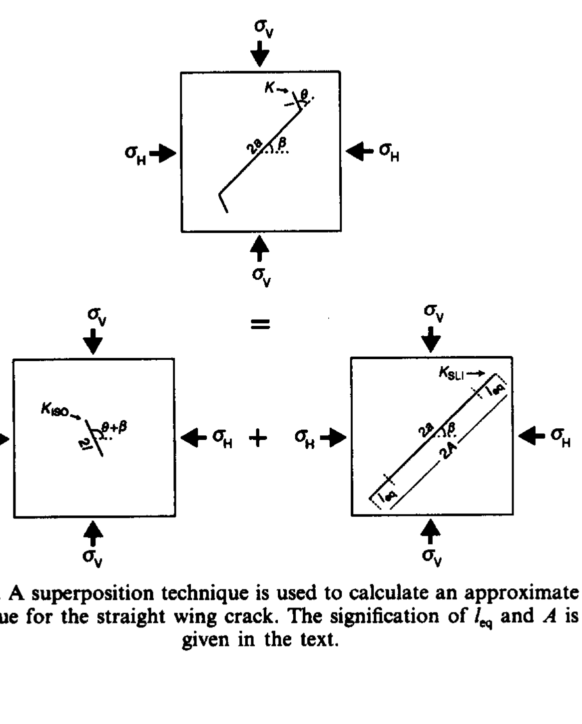

Fig. 3. A superposition technique is used to calculate an approximate $K_{\rm I}$ value for the straight wing crack. The signification of l_{eq} and A is given in the text.

Another simplification is that we use a superposition technique to calculate the $K_{\rm I}$ value for a straight wing crack. We assume that the stress intensity factor $K_{\rm I}$ is the sum of two terms: on one hand a component $K_{\rm ISO}$ for the two straight wing cracks, of common length l, regarded as a single isolated straight crack of length $2l$, and subjected to the external applied stresses; on the other hand a component $K_{\rm SLI}$ due to the stresses induced by the presence of the main crack subjected to the same external stresses (Fig. 3).

If θ is the angle between the wing crack and the main crack, it is easy to show that the first component $K_{\rm ISO}$ is written as:

$$K_{\rm ISO} = \tfrac{1}{2}\{(\sigma_{\rm V} + \sigma_{\rm H}) + (\sigma_{\rm V} - \sigma_{\rm H})\cos 2(\theta + \beta)\}\sqrt{\pi l}. \quad (3)$$

In order to calculate the second component $K_{\rm SLI}$, we use the following procedure. We replace the system (main crack + wing crack pair) by an equivalent single straight crack of length A and same orientation β as the initial main crack (Fig. 3). The length of the equivalent crack is a function of the main crack length a, the wing crack length l and the orientation θ of the wing crack. We assume that this crack is subjected to the same effective shear stress $\sigma_{\rm eff}$ as the main crack, but only over the central part of length $2a$. This results from the fact that on one hand, in compression, it is solely the shearing part of the loading that contributes to $K_{\rm I}$ at the wing crack tip and on the other hand, that the wing crack propagates in such a direction that no shear stress is applied to it, thus its equivalent length $l_{\rm eq}$ on the equivalent straight crack (Fig. 3) should also be seen as shear stress free. In this case it can be shown that the stress intensity factor in mode I corresponding to a straight crack of length $A = a + l_{\rm eq}$ can be written as [12, 13]:

$$K_{\rm I} = 2\sigma_{\rm eff}\sqrt{\frac{a + l_{\rm eq}}{\pi}}\sin^{-1}\left(\frac{a}{a + l_{\rm eq}}\right). \quad (4)$$

We now assume that the wing crack opening is linked to θ. Thus, we multiply $K_{\rm I}$ by an unknown function $f(\theta)$ which is determined by considering the infinitesimal wing crack limit. In this case we identify the solution with the transformed stress intensity factor for wing crack initiation given by equation (2). Thus, we have:

$$K_{\rm SLI} = -3\sigma_{\rm eff}\sqrt{\frac{a + l_{\rm eq}}{\pi}}\sin^{-1}\left(\frac{a}{a + l_{\rm eq}}\right)\sin\theta\cos\frac{\theta}{2}. \quad (5)$$

In order to determine the length $l_{\rm eq}$ of the equivalent wing crack, we use the estimation introduced by Horii and Nemat-Nasser [14] for a long wing crack:

$$K_{\rm I} = -\frac{2a\sigma_{\rm eff}\sin\theta}{\sqrt{\pi l}} \quad (6)$$

which is the mode I stress intensity factor produced by normal splitting forces $F = -2a\sigma_{\rm eff}\sin\theta$ on a crack of length $2l$. Identifying equations (5) and (6) for the long wing crack limit leads to:

$$l_{\rm eq} = \tfrac{9}{4}\, l \cos^2\frac{\theta}{2}. \quad (7)$$

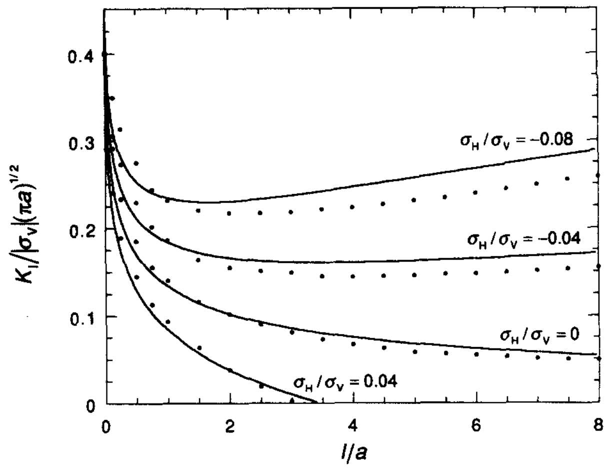

Fig. 4. Normalized stress intensity factor K_I as a function of wing crack length l for indicated σ_H/σ_V with $\mu = 0.3$ and $\beta = 45°$. Solid lines are from the analytic estimate (8) and symbols are for the exact numerical calculation [5].

Finally, by introducing equation (7) into (5) and adding equation (3), we obtain the expression for the mode I stress intensity factor K_I at the tip of the wing crack:

$$K_I = -3\sigma_{eff}\sqrt{\frac{a+l_{eq}}{\pi}}\sin^{-1}\left(\frac{a}{a+l_{eq}}\right)\sin\theta\cos\frac{\theta}{2} + \tfrac{1}{2}\{(\sigma_V+\sigma_H)+(\sigma_V-\sigma_H)\cos 2(\theta+\beta)\}\sqrt{\pi l}. \quad (8)$$

It is interesting to compare our approximate model with the exact solution proposed by Nemat-Nasser and Horii [11], and Horii and Nemat-Nasser [5]. In Fig. 4 we have reported the normalized K_I value for a main crack inclined at $\beta = 45°$, while $\mu = 0.3$ and σ_H varies as indicated on the curves. Symbols represent values from Horii and Nemat-Nasser [5]. It can be seen that our model compares well with the exact solution, especially in the biaxial compression regime ($\sigma_H/\sigma_V \geqslant 0$), but has the advantage of being easily computed, which is not true for the solution proposed by Horii and Nemat-Nasser [5].

COMPARISON WITH PREVIOUS ANALYTICAL MODELS

A number of authors have proposed similar derivations for the K_I in the last decade. We will focus on two of them and show that our model presents advantages, as compared to these previous models. The first derivation has been proposed by Horii and Nemat-Nasser [14], and further applied by Kemeny and Cook [8]. It also relies on a superposition technique and indeed the K_{ISO}-term is exactly the same as the one given in equation (3); but the K_{SLI}-term differs from our derivation [equation (5)] since Horii and Nemat-Nasser [14] introduce an equivalent wing crack length l^* which is determined by the short wing crack limit. They find $l^* = 0.27a$, which does not depend on the wing crack orientation θ, whereas our equivalent wing crack length is a function of θ. Horii and Nemat-Nasser's final formula [14] can thus be written as:

$$K_I = -\frac{2a\sigma_{eff}\sin\theta}{\sqrt{\pi(l+l^*)}} + \tfrac{1}{2}\{(\sigma_V+\sigma_H) + (\sigma_V-\sigma_H)\cos 2(\theta+\beta)\}\sqrt{\pi l}. \quad (9)$$

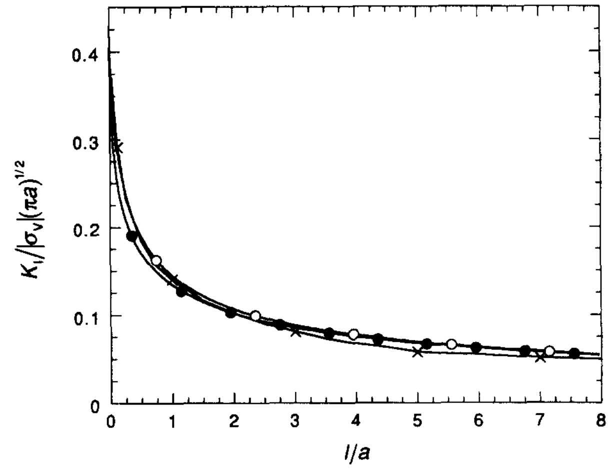

Fig. 5. Normalized stress intensity factor K_I as a function of wing crack length l for a main sliding crack lying at $\beta = 45°$ and subjected to uniaxial compression ($\mu = 0.3$). Comparison between the derivation by Horii and Nemat-Nasser [14] [equation (9), open symbols] and the present derivation [equation (8), closed symbols]. The exact results by Horii and Nemat-Nasser [5] are given for reference (×-symbols).

Figure 5 illustrates the comparison between this derivation and our own calculation for the uniaxial compression case. We see that both models compare very well with the exact calculation by Horii and Nemat-Nasser [5]. However, by comparing equations (8) and (9), it comes out that the main difference lies in the angular dependence of K_I for short wing cracks. Indeed when l is infinitesimally small, equation (9) leads to an angle of initiation $\theta = 90°$, whereas equation (8) leads to $\theta = 70.5°$, which is the value found for crack initiation under mode II conditions [10]. Thus, equation (9) does not lead to the correct θ-value for short wing cracks even if Horii and Nemat-Nasser [14] have derived their l^*-value by using $\theta = 70.5°$ for $l = 0$. This comparison shows that our model may be seen as an improvement of Horii and Nemat-Nasser's model [14] since we have calibrated the θ-dependence of K_I for short wing cracks and the l-dependence for long wing cracks.

We have made a second comparison with an approximate analytical solution given by Ashby and Hallam [7]. These authors propose an approach based on the calculation of energy. Using some approximations and the assumption that the wing crack is straight and parallel to the major compressive stress, their approach leads to an analytical expression for K_I which is written as:

$$K_I = \frac{-\sigma_V\sqrt{\pi a}}{(1+L)^{3/2}}\{1-\lambda-\mu(1+\lambda)-4.3\lambda L\} \times \left\{0.23L + \frac{1}{\sqrt{3}(1+L)^{1/2}}\right\} \quad (10)$$

where $L = l/a$ and $\lambda = \sigma_H/\sigma_V$. This expression does not depend on the orientation of the main crack, which is quite surprising when compared to equations (8) and (9). Since the exact calculation by Horii and Nemat-Nasser [5] has shown that K_I is strongly dependent on the orientation β of the main crack, we cannot use equation (10) and we should rather look at the complete intermediate equation derived by Ashby and Hallam [7] where the angle β has not yet disappeared through the

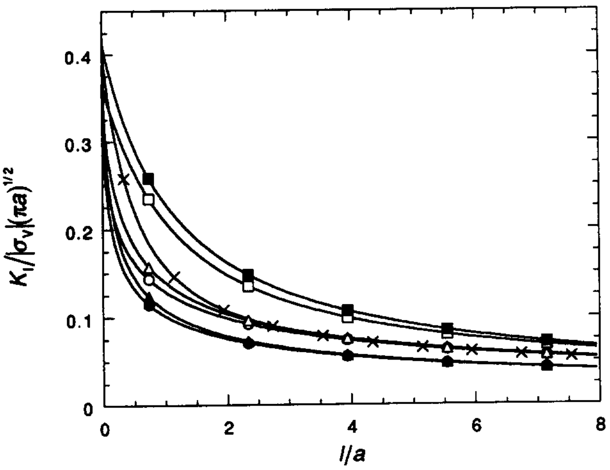

Fig. 6. Normalized stress intensity factor K_I as a function of wing crack length l for two orientations of the main sliding crack (open symbols: $\beta = 40°$; closed symbols: $\beta = 60°$) subjected to a uniaxial compression ($\mu = 0.3$). There is only one curve (×-symbols) for Ashby and Hallam's model [7] since their final result does not depend on β [equation (10)]. Comparison is made with the result by Horii and Nemat-Nasser [14] [△, ▲: equation (9)], the complete intermediate equation by Ashby and Hallam [7] [□, ■: equation (11)], and the present derivation [○, ●: equation (8)].

approximations that these authors apply in their model. This equation may be written as:

$$K_I = \frac{\sqrt{\pi a}}{(1+L)}\left[-\frac{2}{\sqrt{3}}\sigma_{\text{eff}} + \frac{2.5}{\cos\beta}\sigma_H L\right] \times \left[\frac{0.4L\cos\beta\sqrt{1+L} + 1 + L\sin\beta}{\sqrt{\cos^2\beta + (\sin\beta + L)^2}}\right]. \quad (11)$$

Figure 6 illustrates the comparison between equations (8), (9), (10) and (11) for a sliding crack lying at $\beta = 40°$ or 60°, and subjected to uniaxial compression. We see that the final result presented by Ashby and Hallam [7] [equation (10)] is not a correct approximation of K_I, especially for short wing cracks, since it does not account for the dependence of K_I with the orientation β of the main crack. The complete equation derived by Ashby and Hallam [7] [equation (11)] is even less accurate, showing some severe limitations in their approach. The model proposed by Horii and Nemat-Nasser [14] and the present derivation compare well for both angles, and differ mainly on the angle of initiation of the wing crack as discussed earlier.

CONCLUSION

We have developed an original approximation of the stress intensity factor K_I at the wing crack tip which is computed by resolving it into a component K_{ISO} for an isolated straight wing crack and a component K_{SLI} due to the stresses induced by the presence of the main sliding crack. This approximation is consistent with the exact numerical calculation by Horii and Nemat-Nasser [5], and is an improvement of previous derivations, especially without any internal contradiction at the wing crack initiation as may be the case in the model by Horii and Nemat-Nasser [14]. The next important step in our approach will be to introduce crack interactions, and to analyse their effects on the solution we have proposed in this paper.

Acknowledgements—This work has been supported by TOTAL and the GDR 914 (Géomécanique des Roches Profondes) of the CNRS. We thank two anonymous reviewers for their useful comments.

Accepted for publication 1 January 1996

REFERENCES

1. Charlez P. A. *Rock Mechanics, 1, Theoretical Fundamentals*, Editions Technip, Paris (1991).
2. Jaeger J. C. and Cook N. G. W. *Fundamentals of Rock Mechanics*, Chapman and Hall, London (1979).
3. Rudnicki J. W. and Rice J. R. Conditions for the localization of deformation in pressure-sensitive dilatant materials. *J. Mech. Phys. Solids* **23**, 371–394 (1975).
4. Vardoulakis I. Bifurcation analysis of the triaxial test on sand samples. *Acta Mech.* **32**, 35–54 (1979).
5. Horii H. and Nemat-Nasser S. Compression-induced microcrack growth in brittle solids: axial splitting and shear failure. *J. Geophys. Res.* **90**, 3105–3125 (1985).
6. Costin L. S. Damage mechanics in the post-failure regime. *Mech. Mater.* **4**, 149–160 (1985).
7. Ashby M. F. and Hallam S. D. The failure of brittle solids containing small cracks under compressive stress states. *Acta metall.* **34**, 497–510 (1986).
8. Kemeny J. M. and Cook N. G. W. Crack models for the failure of rocks in compression. In *2nd Int. Conf. Constitutive Laws for Engng. Materials*, pp. 879–887. Tucson (1987).
9. Lawn B. *Fracture of Brittle Solids*, Second edition, Cambridge University Press, Cambridge (1993).
10. Cotterell B. and Rice J. R. Slightly curved or kinked cracks. *Int. J. Fract.* **16**, 155–169 (1980).
11. Nemat-Nasser S. and Horii H. Compression-induced nonplanar crack extension with application to splitting, exfoliation, and rockburst. *J. Geophys. Res.* **87**, 6805–6821 (1982).
12. Sih G. C. and Liebowitz H. Mathematical theories of brittle fracture. In *Fracture, 2, Mathematical Fundamentals* (Edited by Liebowitz, H.), pp. 67–190. Academic Press, New York (1968).
13. Bui H. D. *Mécanique de la Rupture Fragile.* Masson, Paris (1978).
14. Horii H. and Nemat-Nasser S. Brittle failure in compression: splitting, faulting and brittle-ductile transition. *Phil. Trans. R. Soc. Lond. A.* **319**, 337–374 (1986).